CHEMISTRY OF MATERIALS

Article

pubs.acs.org/cm

# Understanding the Chemical Stability of Polymers for Lithium−Air Batteries

Chibueze V. Amanchukwu,[†] Jonathon R. Harding,[†] Yang Shao-Horn,*[,‡,§] and Paula T. Hammond*[,†]

[†]Department of Chemical Engineering, [‡]Department of Mechanical Engineering, and [§]Department of Materials Science and Engineering, Massachusetts Institute of Technology, Cambridge, Massachusetts 02139, United States

Supporting Information

**ABSTRACT:** Recent studies have shown that many aprotic electrolytes used in lithium−air batteries are not stable against superoxide and peroxide species formed upon discharge and charge. However, the stability of polymers often used as binders and as electrolytes is poorly understood. In this work, we select a number of polymers heavily used in the Li−air/Li-ion battery literature, and examine their stability, and the changes in molecular structure in the presence of commercial $Li_2O_2$. Of the polymers studied, poly(acrylonitrile) (PAN), poly(vinyl chloride) (PVC), poly(vinylidene fluoride) (PVDF), poly(vinylidene fluoride-*co*-hexafluoropropylene) (PVDF-HFP), and poly(vinylpyrrolidone) (PVP) are reactive and unstable in the presence of $Li_2O_2$. The presence of the electrophilic nitrile group in PAN allows for nucleophilic attack by $Li_2O_2$ at the nitrile carbon, before further degradation of the polymer backbone. For the halogenated polymers, the presence of the electron-withdrawing halogens and adjacent $\alpha$ and $\beta$ hydrogen atoms that become electron-deficient due to hyperconjugation makes PVC, PVDF, and PVDF-HFP undergo dehydrohalogenation reactions with $Li_2O_2$. PVP is also reactive, but with much slower kinetics. On the other hand, the polymers poly(tetrafluoroethylene) (PTFE), Nafion, and poly(methyl methacrylate) (PMMA) appear stable against nucleophilic $Li_2O_2$ attack. The lack of labile hydrogen atoms and the poor leaving nature of the fluoride group allow for the stability of PTFE and Nafion, while the methyl and methoxy functionalities in PMMA reduce the number of potential reaction pathways for $Li_2O_2$ attack in PMMA. Poly(ethylene oxide) (PEO) appears relatively stable, but may undergo some cross-linking in the presence of $Li_2O_2$. Knowledge gained from this work will be essential in selecting and developing new polymers as stable binders and solid or gel electrolytes for lithium−air batteries.

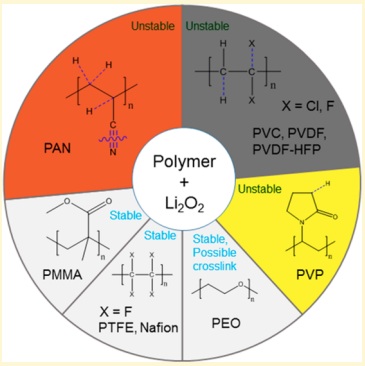


## INTRODUCTION

Innovations in portable electronic devices such as smart phones and laptops, and electrical vehicles, can be partly attributed to lithium-ion batteries, the most energy-dense batteries commercially available.[1,2] Lithium-ion battery use in electric vehicles has allowed for the gradual electrification of transport, but the current format, graphitic negative electrode and transition metal oxide positive electrode, has reached its practical limits in gravimetric energy density.[1−3] To allow future electric vehicles to effectively compete with gasoline-powered cars in driving range per charge, newer battery chemistries with much higher energy densities are being explored. In recent years, lithium−air ($O_2$) batteries have emerged as a possible lithium-ion replacement because their theoretical gravimetric capacity (3861 mAh/$g_{Li}$) is an order of magnitude greater than lithium-ion (372 mAh/$g_C$) if a lithium metal negative electrode is utilized as opposed to a graphitic intercalation electrode.[1,4−8] Although this difference has spurred intense research and commercial interest, several challenges such as electrolyte instability,[9−11] low rate-capability,[12] poor round-trip efficiency,[10,12,13] and limited cycle life[13,14] must be addressed before possible commercialization.

In its current configuration, lithium−air ($O_2$) battery technology uses lithium metal as the negative electrode, a porous high surface area material (e.g., carbon) as the positive electrode, and oxygen as the active material.[1,3] During cell discharge, oxygen is reduced to form superoxide radical anions ($O_2^{\bullet-}$)[15] that can combine with lithium ions to form lithium superoxide ($LiO_2$)[15,16] before the formation of the desired discharge product, lithium peroxide ($Li_2O_2$).[4,15−17] During charging, lithium peroxide is then oxidized to evolve oxygen.[15,16,18,19] The reversible formation and oxidation of lithium peroxide is therefore vital to the rechargeable nature of a lithium−air cell.[14,18,20]

Reduced oxygen species such as the superoxide radical anion are highly reactive species,[21] and the desired discharge product, lithium peroxide, is a strong base[22] that can participate in unwanted side reactions detrimental to cell performance.[11] These superoxide and peroxide species readily decompose carbonate-based electrolytes, such as ethylene and propylene carbonate, that are widely used in commercial lithium-ion batteries,[23] and even prevent the formation of $Li_2O_2$, instead leading to side products such as lithium carbonate and lithium formate.[10,23,24] Ether-based electrolytes (e.g., 1,2-dimethoxy-

Received: October 29, 2014
Revised: December 5, 2014
Published: December 5, 2014

  

DOI: 10.1021/cm5040003
*Chem. Mater.* 2015, 27, 550−561

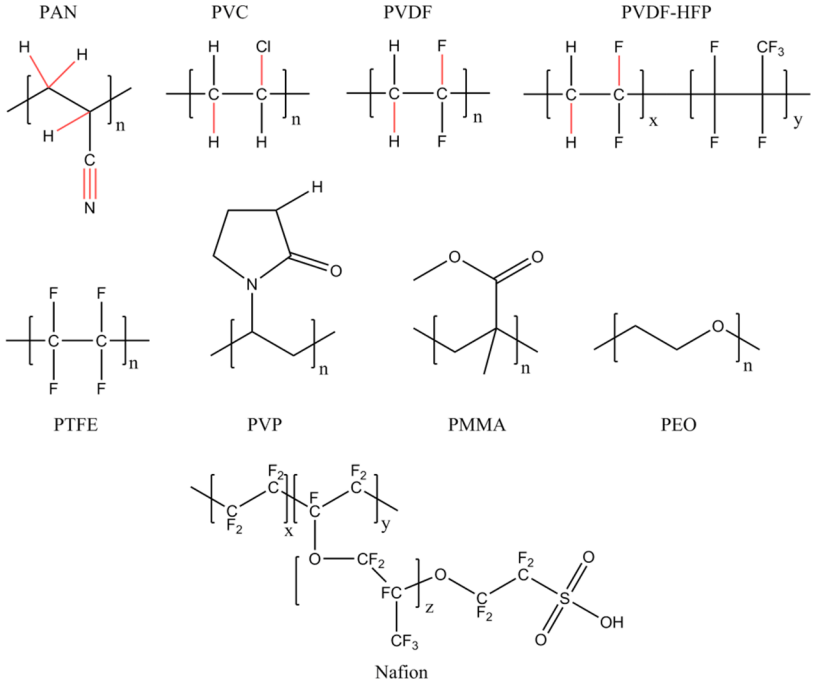


**Figure 1.** List of polymers studied for this work. The red lines represent bonds that are cleaved during reaction with $Li_2O_2$.

ethane and tetraglyme) have proven more stable than their carbonate counterparts and allow for the formation of $Li_2O_2$ during the first discharge; however, these ether-based electrolytes also decompose upon further cell cycling.[9,11] Other electrolyte systems such as amides[25] and DMSO[26] have been explored, but they too decompose during cell cycling and on exposure to $Li_2O_2$ and $KO_2$,[27] highlighting the importance of developing stable electrolytes.

In addition to Li−air battery research into liquid aprotic electrolytes, Li−air cells with polymer electrolytes have been explored.[1,28,29] Some of the widely used polymer electrolytes are stable in contact with lithium metal, and, like their ceramic counterparts, can help suppress lithium dendrite formation.[30] In addition, polymers have been widely used as binder for the oxygen electrode.[9,12,14,20,25,29] Therefore, the ubiquity of polymers in lithium−air research, and the technological potential of new roles for polymers as solid-state electrolytes are developed, necessitate a thorough study to carefully evaluate their stability when exposed to the discharge and charge cell reactions.

Recent work by several researchers has highlighted the importance of evaluating the stability of polymers for lithium−air use. Black et al. studied the decomposition of the common binder poly(vinylidene fluoride), and reported on the dehydrofluorination of the polymer backbone in the presence of chemically generated $LiO_2$, and the formation of lithium fluoride (LiF) during cell discharge.[31] Nasybulin et al. studied a wider range of polymers, and characterized their stability in the presence of $KO_2/Li_2O_2$ based on the formation of inorganic decomposition products such as $K_2CO_3$.[32] However, indicating the formation of inorganic decomposition products like $K_2CO_3$ does not give insight into how the polymer chemical structure reacts. Therefore, it is not known how the polymeric structures of PAN, PVC, PVP, etc., react or are affected by the presence of $Li_2O_2$. Are the resultant carbonates observed using X-ray diffraction (XRD) due to a degrading polymeric backbone or the polymeric functional group? Although the mechanism of PVDF degradation in lithium−air has been studied by some researchers,[29,31] there is a dearth in knowledge about the mechanism of degradation for other polymers. Despite these previous works, it is not known what functional groups should be avoided to prevent reactivity with lithium peroxide, and in turn how to inhibit reactivity of these polymers. This work strives to address these issues. There remains a need for greater insights into how and why the polymers react with $Li_2O_2$, the functional groups and polymer backbones that are especially susceptible to attack, the extent and time frame (days, weeks, etc.) of polymer degradation, and some controlling trends and principles that govern polymer reactivity and instability that can inspire new stable polymer binders and electrolytes.

In this work, we aim to address some of these questions by evaluating the reactivity and stability of a subset of polymers in the presence of commercial lithium peroxide powder. Because the desired discharge product of a lithium−air cell is lithium peroxide, it is vital that the polymer used be stable in contact against $Li_2O_2$. Using commercial $Li_2O_2$ affords us a quick screening tool to deduce the chemical stability of a polymer or small organic molecule before complete lithium−air cells are fabricated. In addition, it isolates the polymer and eliminates the influence of lithium metal and carbon in the oxygen electrode as it pertains to reactivity against products formed upon discharge and charge in Li−air batteries.[11,13,33] For this Article, we chose to examine a set of polymers that have been thoroughly studied in the lithium-ion and lithium−air literature, the structures of which are shown in Figure 1.[30,32,34,35] These polymers have aliphatic C−C backbones (except poly(ethylene oxide)), and their side-chain functionalities were chosen to understand the influence of the side-chain functional groups on the reactivity and stability of the polymer and its backbone. In addition to determining the stability of each polymer tested, we establish reactivity trends across all evaluated polymers with regard to the electron-withdrawing/electron-donating nature of their functional groups, the influence of $\alpha$- and $\beta$-hydrogen atoms in the hydrocarbon polymer backbone, and how these


DOI: 10.1021/cm5040003
Chem. Mater. 2015, 27, 550−561

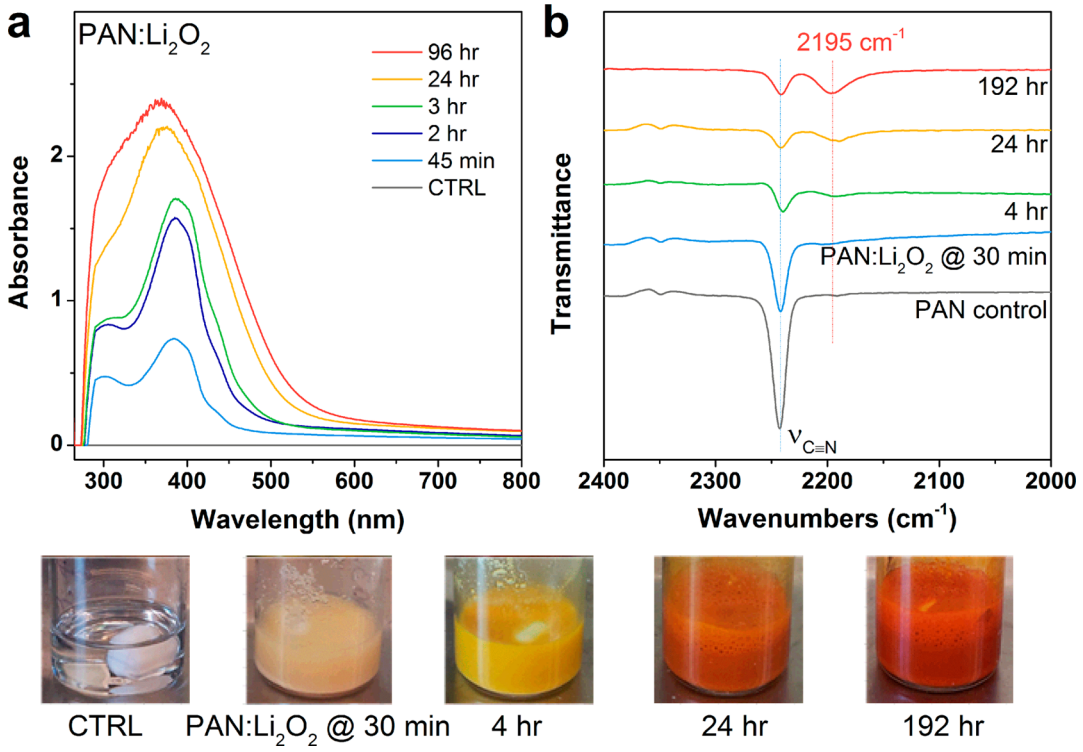


**Figure 2.** (a) UV–vis spectra for the reaction of PAN with $Li_2O_2$. The rise in absorbance in (a) corresponds to the rise in the concentration of soluble decomposition species due to PAN degradation. (b) FTIR spectra for the reaction of PAN with $Li_2O_2$, which shows a decrease in the nitrile stretching vibration (2242 $cm^{-1}$) and the rise of a new peak at 2195 $cm^{-1}$ due to PAN reaction that has previously been attributed to a $\beta$-amino nitrile.[38] The reaction pictures correspond to the same samples used to obtain the FTIR spectra.

factors contribute to the polymers' chemical stability in lithium–air. Knowledge and reactivity patterns gained from this work should prove critical in the bottom-up design of new polymers to serve as binders and mechanical supports, or as solid-state/gel polymer electrolytes for future lithium–air batteries.

## EXPERIMENTAL SECTION

**Materials Used.** All polymers used in this work are shown in Figure 1, and an explanation of the abbreviations is listed in the Abbreviations section. The polymers PAN, PMMA, PTFE, PVC, PVDF, and PVDF-HFP were obtained from Sigma-Aldrich. PEO was obtained from Polysciences, Inc. Nafion was obtained from Ion Power Inc. as a 7.2 wt % lithiated Nafion in isopropanol solution. Drops of the Nafion solution were drop-cast onto a polystyrene weigh-boat and allowed to slowly evaporate overnight. The resultant film was vacuum-dried at 50 °C for at least 24 h. Lithium peroxide ($Li_2O_2$) powder (technical grade, 90%), anhydrous *N*,*N*-dimethylformamide (DMF), and *N*,*N*-dimethylacetamide (DMAc) were purchased from Sigma-Aldrich, and used as obtained. Deuterated DMSO (D, 99.9%) and deuterated DMSO with tetramethylsilane (D, 99.9% + 0.05% v/v TMS) were obtained from Cambridge Isotope Laboratories, Inc.

**Chemical Reactivity Tests.** All chemical reactivity tests were performed in a dry-nitrogen glovebox (MBRAUN, $H_2O$ < 0.1 ppm, $O_2$ < 10 ppm). The following describes a typical experiment. In a 20 mL vial, about 132 mg of polymer was dissolved in 4 mL of DMF. Because no solvent has been proven to be completely stable in lithium–air, DMF was chosen to serve as our reaction medium. While DMF can be unstable when used in a lithium–air cell,[25] it is used because its FTIR and UV–vis peaks mostly do not interfere with the peaks of interest in the studied polymers (Supporting Information Figure S9), and it allows for the use of a DMF-based gel permeation chromatography (GPC) instrument. For PVDF only, DMAc was used as the solvent because PVDF is insoluble in DMF. The polymer/solvent mixture was stirred to allow the polymer to dissolve. In another 20 mL vial, about 85 mg of $Li_2O_2$ was added to allow for an excess mass concentration of $Li_2O_2$ as compared to the polymer mass concentration. Next, 1.5 mL of the polymer/solvent solution was added to the vial containing $Li_2O_2$. The mixture was stirred throughout the course of the experiment.

**FTIR Characterization.** In the glovebox, 10 $\mu$L of the polymer/$Li_2O_2$/solvent mixture was placed on a transparent IR card (International Crystal Laboratories, 19 mm KBr aperture IR card). The IR card containing sample was allowed to rest in the glovebox to allow for solvent evaporation until there was no visible trace of solvent. However, some of the samples were also transferred to the glovebox ante-chamber, where it was allowed to vacuum-dry at room temperature for at least 2 days for effective solvent removal. The IR card was then transferred out of the glovebox, and the IR spectra were obtained immediately. A JASCO 4100 Fourier transform infrared (FTIR) spectrometer was used for data collection. All spectra were obtained in absorbance mode with a resolution of 1 $cm^{-1}$, using 100 accumulation scans. The spectrometer was flushed with dry nitrogen before and during sample measurement.

**UV–Vis Characterization.** In a 20 mL vial, a polymer was dissolved in DMF (or DMAc for PVDF) to obtain a 10.5 mg/mL mass concentration of polymer. 100 $\mu$L of the polymer/solvent solution was removed to serve later as a control. Next, $Li_2O_2$ powder was added to the polymer solution to obtain a $Li_2O_2$ concentration of 16.4 mg/mL. The mixture was thoroughly stirred throughout the course of the experiment. At different time points, stirring was stopped and the mixture was allowed to rest for about 15 min to ensure that the dispersed $Li_2O_2$ fell out of solution. For example, for the "1 h" time point, stirring was stopped at 45 min. Carefully, a volumetric pipet was used to collect 25 $\mu$L of the topmost part of the mixture (to ensure $Li_2O_2$ particles are also not collected), and deposited in an empty 3 mL vial. Next, 1 mL of pure DMF was added to dilute the contents of the 3 mL vial. The vial was vigorously shaken to ensure full dissolution. A Pasteur pipet was then used to transfer the diluted mixture to a UV–vis cuvette. The pure solvent (DMF or DMAc) was used as a blank. A Beckman Coulter DU 800 ultraviolet–visible (UV–vis) spectropho-


DOI: 10.1021/cm5040003
*Chem. Mater.* 2015, 27, 550–561

tometer was used for data collection. For data analysis, the CTRL data, which corresponded to the polymer/solvent control, were subtracted from each polymer/$Li_2O_2$/solvent time point to better illustrate the accumulation of decomposition species as a function of time. In addition, the CTRL data were also subtracted, leading to the straight line that corresponds to zero in the UV−vis spectra.

*Details.* (a) For PAN, 5 $\mu$L of the PAN/$Li_2O_2$/DMF mixture was used (instead of 25 $\mu$L) because of the very high concentration of decomposition species, and diluted with 1 mL of DMF. (b) For PVDF-HFP and PVC, 25 $\mu$L of the polymer/$Li_2O_2$/DMF mixture was used and diluted with 1 mL of DMF. (c) For PVDF, a syringe was used to collect about 0.2 mL of the PVDF/$Li_2O_2$/DMAc mixture and filtered using a 0.45 $\mu$m Teflon filter into a polystyrene well plate. Next, 25 $\mu$L of the contents of the well plate was then transferred to a 3 mL vial and diluted with 1 mL of DMAc. The PVDF mixture was filtered because of the interference of $Li_2O_2$ particles during data collection. (d) For Nafion and PVP, the polymer/$Li_2O_2$/DMF mixture was also filtered in the same manner as PVDF, and 25 $\mu$L of the mixture was diluted with 1 mL of DMF. (e) For the CTRL data for each polymer, the same volume used for the polymer/$Li_2O_2$ mixture was used. For example, 5 $\mu$L of the PAN/DMF mixture (without $Li_2O_2$) was diluted with 1 mL of DMF to obtain the CTRL data.

**NMR Characterization.** In a 5 mL vial, about 16 mg of polymer was dissolved in 1 mL of deuterated DMSO with TMS (D, 99.9% + 0.05% v/v TMS). Next, 0.5 mL of the polymer solution was transferred to a NMR tube for $^1$H NMR analysis. This served as the control. In another 5 mL vial, about 30 mg of $Li_2O_2$ was dissolved in 0.7 mL of deuterated DMSO without TMS (D, 99.9%). Next, 0.4 mL of the $Li_2O_2$/DMSO dispersion was added to the NMR tube containing the polymer solution. The NMR tube was sonicated throughout the experiment to keep the $Li_2O_2$ particles dispersed in solution. At different time points, the NMR tube was removed from the sonication bath and taken for $^1$H NMR analysis. The maximum temperature reached in the sonication bath was 50 °C. Although the temperature in the sonication bath can go as high as 50 °C, it was not held at 50 °C throughout the course of sonication. Because the results obtained using NMR are consistent with the FTIR and UV−vis data, the temperature rise in the sonication bath is not believed to affect the interpretation of our results. All measurements (except $^1$H NMR and sonication bath) were performed in a nitrogen-filled glovebox ($H_2O$ < 0.1 ppm, $O_2$ < 10 ppm). The contents of the NMR tube were never exposed to the atmosphere. A Bruker AVANCE and Bruker AVANCE III-400 MHz nuclear magnetic resonance (NMR) spectrometer was used.

**GPC Characterization.** A DMF-based Waters gel permeation chromatography (GPC) instrument was used to determine the polymer molecular weight before and after reaction with $Li_2O_2$. The polymer/$Li_2O_2$/DMF mixture was filtered using a 0.45 $\mu$m Teflon filter before GPC analysis. A poly(methyl methacrylate) calibration standard was used.

## RESULTS AND DISCUSSION

**Poly(acrylonitrile).** Poly(acrylonitrile) (PAN) has been a widely used mechanical support for gel polymer electrolytes, and PAN support/electrolyte systems have had some of the highest reported ionic conductivities.[36] In addition, PAN was the polymer of choice for the first lithium−air cell developed by Abraham et al.[35] In our work, PAN was found to be highly unstable, and reacted readily with $Li_2O_2$. Using procedures detailed in the Experimental Section, commercial lithium peroxide was added to a PAN/dimethylformamide (DMF) solution, and within minutes, the previously clear and transparent solution turned yellow (Figure 2). After 1 day, the solution deepened to an orange color, and finally to a permanent dark red hue after about 2 days. The color changes are an obvious indication of a chemical reaction between PAN and $Li_2O_2$. Several characterization techniques such as ultraviolet−visible (UV−vis) spectroscopy, Fourier transform infrared (FTIR) spectroscopy, nuclear magnetic resonance (NMR), and gel permeation chromatography (GPC) were used to characterize the decomposition products and elicit the mechanism and rate of PAN reaction.

Because the solution color changes are due to resultant soluble decomposition species, absorption in the ultraviolet−visible (UV−vis) region can be particularly helpful in monitoring the reaction. Therefore, the reaction mixture of PAN/$Li_2O_2$/DMF was carefully studied using UV−vis, and Figure 2a shows an increase in the absorbance of the soluble decomposition species as a function of $Li_2O_2$ exposure time. Beer's law allows for the correlation of absorbance with concentration;[37] therefore, the absorbance increase corresponds to an increase in concentration of soluble decomposition species with time. Although Beer's law does have a concentration limitation, the overall trends discussed here are still valid within the absorbance range of 0−1, for which Beer's law is most accurate. These decomposition species could only result from the chemical degradation of PAN by $Li_2O_2$. After about 3 days, the saturation or completion of the reaction was reached, and the concentration of decomposition species approached steady state in solution. In addition, the loss of the absorbance peak at 310 nm corresponds to the conversion of an intermediate decomposition species to another, and there were slight shifts of the wavelength of maximum absorbance ($\lambda_{max}$) as the reaction proceeded. We further used FTIR and NMR to understand the molecular changes in the PAN structure to provide valuable information that can be used to devise methods to mitigate reaction or avoid the functionality responsible for reaction.

We propose that the reactive chemical functionality in PAN is the nitrile functional group (−C≡N). The nitrile functional group is highly polarized, meaning the carbon directly attached to the nitrogen has a partial positive character ($\delta^+$), and is electrophilic.[37] Fortunately, this functional group has a separate and highly definitive stretching vibration at 2242 cm$^{-1}$, making FTIR[39] an easy technique for characterization and possible delineation of the reaction mechanism. This hypothesis is supported by FTIR measurements in Figure 2b, which show a consistent decrease in the intensity of the nitrile functional group as $Li_2O_2$ exposure time increases. This observation suggests that $Li_2O_2$ attacks the nitrile functionality, which leads to imine-like conjugated soluble species (−C═N−C═N−) that are responsible for the marked color changes observed visually and monitored in UV−vis.[38,40,41] The observed wavelengths of these imine species are dependent on the cause of PAN decomposition. For thermolysis of PAN under vacuum at 150 °C, and thermo-oxidation in the presence of atmospheric $O_2$, two absorption bands attributed to polyimine appear in the UV−vis spectra at 270 and 360 nm (thermolysis), and 270 and 385 nm (thermo-oxidation), respectively.[42] At early decomposition times (at least 3 h), two absorption bands are present at 310 and 385 nm that may be due to these polyimine species. For much later decomposition times, the absorption spectrum widens, consolidating the two maxima, and the $\lambda_{max}$ shifts to lower wavelengths, an indication of a variation in the level of conjugation and/or oxidation of the polyimine species.[42] As a result of the electrophilic carbon atom in the nitrile functional group, nitriles can undergo nucleophilic addition, and are susceptible to oxygen radical attack from radicals generated by $Li_2O_2$.[37]

Interestingly, when a stoichiometric excess of $Li_2O_2$ was used (excess mole ratio of peroxide to nitrile repeat unit), a new IR


DOI: 10.1021/cm5040003
Chem. Mater. 2015, 27, 550−561

absorption peak at 2195 $cm^{-1}$ appeared after about 4 h and increased in intensity as the reaction proceeded.[38] The observed color changes, the decrease in nitrile functionality, and subsequent increase in the new functional group at 2195 $cm^{-1}$ (attributed by Coleman et al. to be a $\beta$-amino nitrile)[38] have previously been observed during the thermal degradation of PAN at 200 °C and reduced pressure,[38] and also during benzoic acid treatment at 170 °C.[40] Therefore, it is interesting to note that similar changes were observed during $Li_2O_2$ exposure at room temperature, suggesting that the reaction with free radicals derived from peroxide yields some degree of nitrile oligomerization at much lower temperatures than previously reported. Although excess $Li_2O_2$ concentration was used, the nitrile functional group was not completely eliminated based on FTIR (which could be due to the presence of short nitrile oligomers), and it took about 3 days for the reaction to equilibrate and reach saturation. In addition, if the PAN/$Li_2O_2$/DMF mixture was not stirred thoroughly, a highly viscous dark red gel was found, possibly resulting from cross-linking due to the generated imine groups and the formation of conjugated ladder-like structures often observed as precursors to graphitization.[43]

To determine the extent of reaction on the polymer backbone, we used $^1$H NMR to monitor the aliphatic $CH_2$ hydrogen atoms in the main polymer backbone and the $\alpha$-CH hydrogen directly attached to the nitrile group. Figure 3 shows the $^1$H NMR spectra chronicling the reaction of PAN. After about 4 h, new proton peaks arose, whose source can only be from the protons available in the polymer backbone. After 3 days, the $\alpha$-CH ($\delta$ = 3.2 ppm) and $\beta$-$CH_2$ ($\delta$ = 2.1 ppm) proton signals were almost nonexistent, implying they were cleaved and the polymer backbone significantly degraded. Also, there was the rise of a new peak at $\delta$ = 2.95 ppm that has previously been observed in colored PAN (obtained through thermal treatment or treatment with base),[41] and ascribed to methylene and/or methine protons resulting from cyclic ladder-like decomposition species or azomethine structures.[41] Incomplete PAN reaction, the presence of protons in very different chemical environments along the chemical backbone, and other smaller oligomers that may form during degradation led to the conglomeration of peaks from $\delta$ = 0.5−2.4 ppm. In addition, these new proton peaks could also be due to protons on the end groups of polymers that have been cleaved. Gel permeation chromatography (GPC) data allowed us to monitor the changes in the polymer molecular weight, and we observed a 65% decrease in the weight-average molecular weight of the polymer, further supporting polymer degradation and breakdown.[40]

Several researchers have proposed decomposition mechanisms for the degradation of PAN, and the mechanism that best correlates with our experimental results is that by Coleman et al.[38] for thermal degradation of PAN. The mechanism is adapted and reproduced in Supporting Information Figure S1. First, as shown in the FTIR spectra (Figure 2b), reaction begins by nucleophilic attack at the carbon of the nitrile functional group by dispersed $Li_2O_2$ particles or the peroxide anion (if $Li_2O_2$ slightly dissociates in DMF). There is a subsequent decrease in nitrile functionality within 4 h, and formation of imine-like (−C═N) ionic species responsible for the yellowish color, further confirmed by the two absorption bands in the UV−vis spectra as mentioned previously. The nitrile functional group is highly electron-withdrawing, meaning that the $\alpha$-CH carbon atom becomes electron deficient due to an inductive

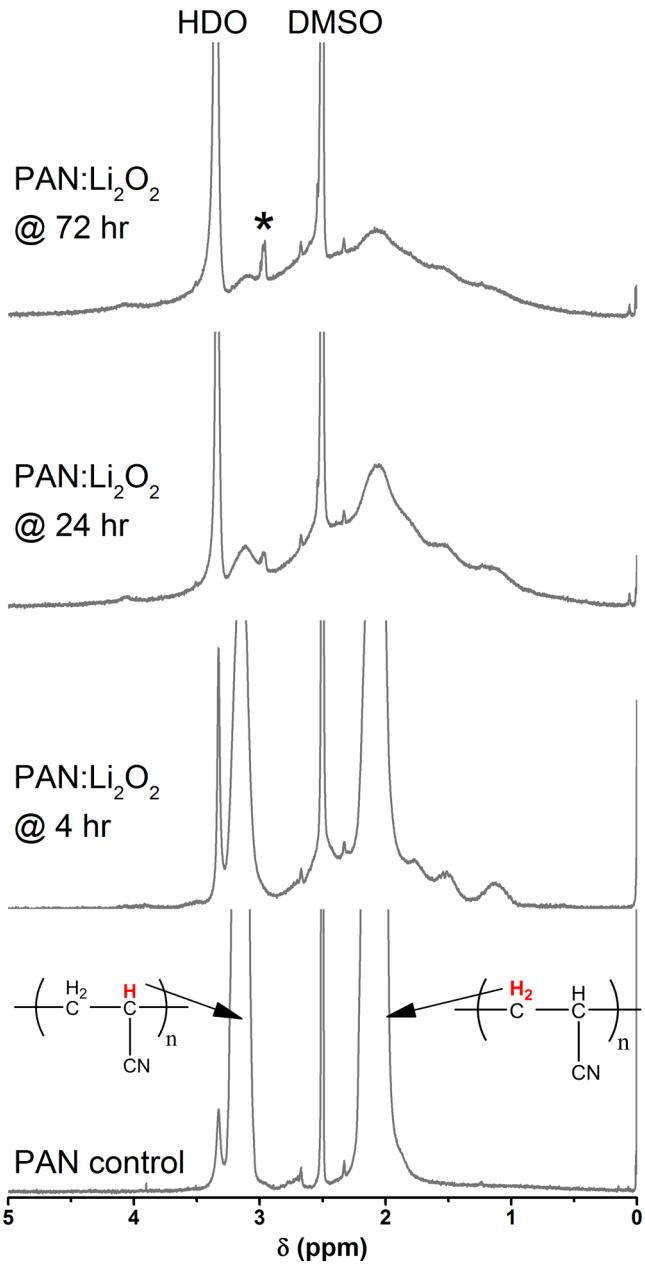


**Figure 3.** $^1$H NMR (400 MHz; DMSO; $Me_4Si$) spectra of PAN reaction with $Li_2O_2$. As reaction time increases, there is a loss of the $\alpha$-CH ($\delta$ = 3.2 ppm) and $\beta$-$CH_2$ protons ($\delta$ = 2.1 ppm) in the molecular structure of PAN due to reaction with $Li_2O_2$. The HDO peak is present because pure deuterated DMSO contains $H_2O$ residue, which can exchange protons with DMSO. The rise in the HDO concentration can be due to the reaction of $Li_2O_2$ with DMSO, which several authors have postulated can lead to the formation of water.[26,27] *New peak at $\delta$ = 2.95 ppm that has been previously observed in colored PAN.[41]

electron withdrawing effect, and, more importantly, the $\alpha$-CH hydrogen atom becomes electron deficient due to hyperconjugation.[37] Hence, the $\alpha$-CH hydrogen atoms are acidic and vulnerable to nucleophilic attack from $O_2^{2-}$ or, more probably, the newly formed and more nucleophilic imine ions.[38] Therefore, after 4 h of reaction, the $\alpha$-CH proton signals (using $^1$H NMR) begin to decrease in intensity, leading to a different conjugated species (−C═C−N) that is responsible for the second color change from yellow to orange, and


DOI: 10.1021/cm5040003
Chem. Mater. 2015, 27, 550−561

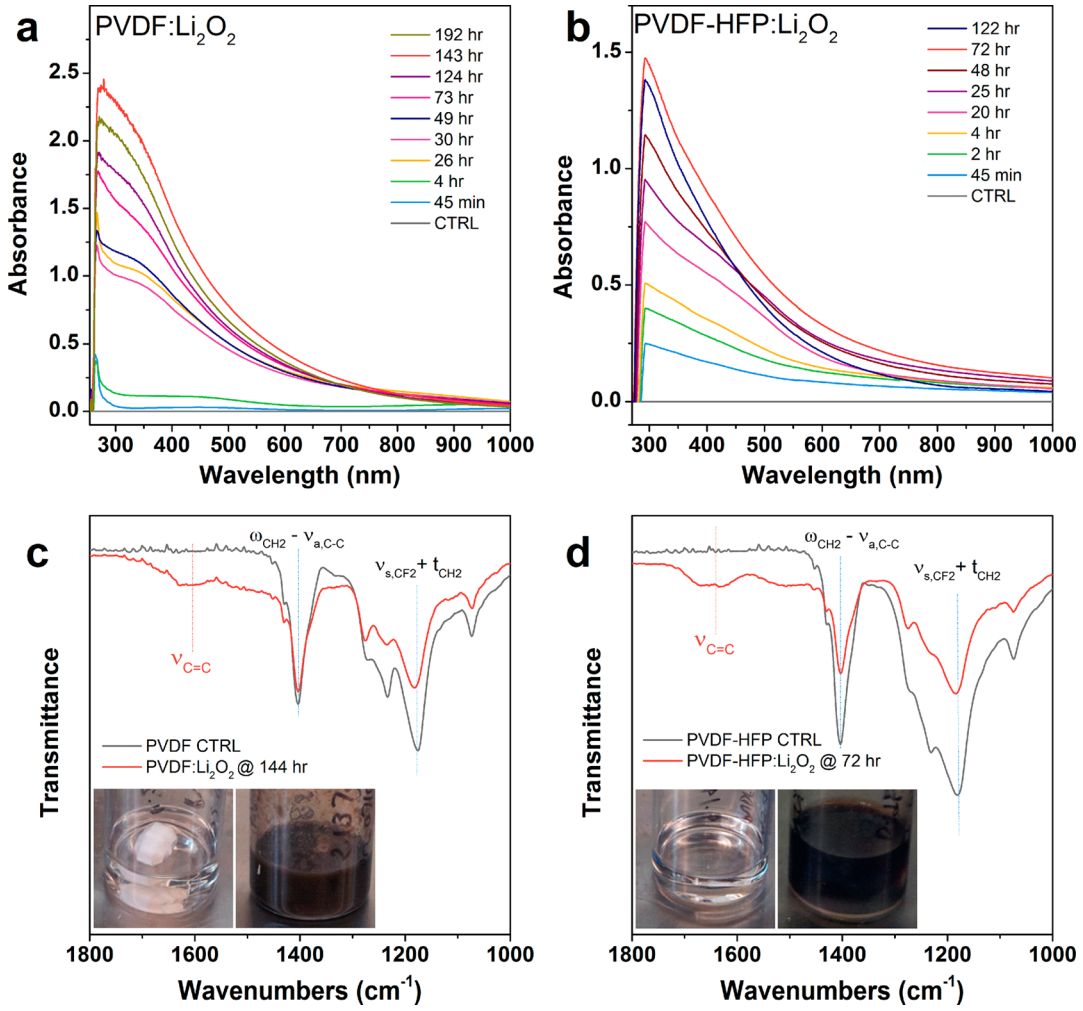


**Figure 4.** UV−vis spectra of the reaction of (a) PVDF and (b) PVDF-HFP with $Li_2O_2$ as a function of time. The absorbance increase in the UV−vis spectra shows the rise in concentration of soluble decomposition species resulting from PVDF and PVDF-HFP degradation. (c) FTIR spectra of the PVDF:$Li_2O_2$ reaction after 144 h and (d) the PVDF-HFP:$Li_2O_2$ reaction after 72 h. The rise of the C=C stretching vibrations around 1650 $cm^{-1}$ confirms the formation of conjugated alkene-like degradation products whose formation is tracked in the UV−vis spectra. The inset pictures in (c) and (d) correspond to the PVDF and PVDF-HFP solutions after reaction with $Li_2O_2$, respectively. Peak assignments and vibration descriptors are consistent with those of ref 47.

possibly responsible for the disappearance of the ultraviolet peak at 310 nm, and the distinct difference between the UV−vis spectra at 3 h and the UV−vis spectra at 19 h (Figure 2a). Finally, once the electron-deficient $\beta$-$CH_2$ protons and $\alpha$-CH protons are cleaved, the final solution becomes dark red. On the basis of these results, PAN is unsuitable for use in Li−air batteries due to its high reactivity and almost complete degradation in the presence of $Li_2O_2$.

**Halogenated Polymers.** Of the polymers heavily utilized in the battery literature, halogenated polymers are often at the forefront with some like poly(vinylidene fluoride) (PVDF), sold under the trademark Kynar, that are commercially marketed for battery applications. Similar to poly(acrylonitrile), halogenated polymers such as poly(vinyl chloride) (PVC), PVDF, poly(vinylidene fluoride-*co*-hexafluoropropylene) (PVDF-HFP), and Nafion have been used as mechanical supports for gel polymer electrolytes,[29,30] but even more so as binders for the positive electrode.[9,12,14] In contrast, poly(tetrafluoroethylene) (PTFE), commonly known as Teflon, is almost exclusively used as a binder for lithium-battery applications.[20,25] These halogenated polymers are mechanically robust,[30] but despite the presence of the strong carbon−halogen bonds, PVC, PVDF, and PVDF-HFP are unstable and react readily with $Li_2O_2$. On the other hand, Nafion and PTFE are stable and do not appear to react with $Li_2O_2$.

When $Li_2O_2$ powder was added to the PVC/DMF solution, the solution color changed immediately from transparent to slight orange, before becoming a dark mixture within 3 days (Figure 5b). Similar color changes occurred for PVDF and PVDF-HFP when $Li_2O_2$ powder was added with both changing from clear solutions to black within 3 days (Figure 4c,d), indicative of the instability of these polymers. This finding agrees with recent work by Black et al.[31] and others studying PVDF,[32,44] and past work that has shown strong bases such as potassium hydroxide (KOH) can act as a dehydrochlorination agent.[45,46] For lithium−air, these bases can be $O_2^{\bullet-}$, $LiO_2$, $Li_2O_2$, etc.; this work primarily focuses on $Li_2O_2$.

The changes in color and formation of possible $\pi$-conjugated species again allowed for the use of UV−vis spectroscopy to track the reactivity of PVC, PVDF, and PVDF-HFP in contact with $Li_2O_2$ (Figures 4a,b, 5a).[37] As the polymer/$Li_2O_2$ exposure time increased, so did the absorption in the UV−vis spectra,


DOI: 10.1021/cm5040003
Chem. Mater. 2015, 27, 550−561

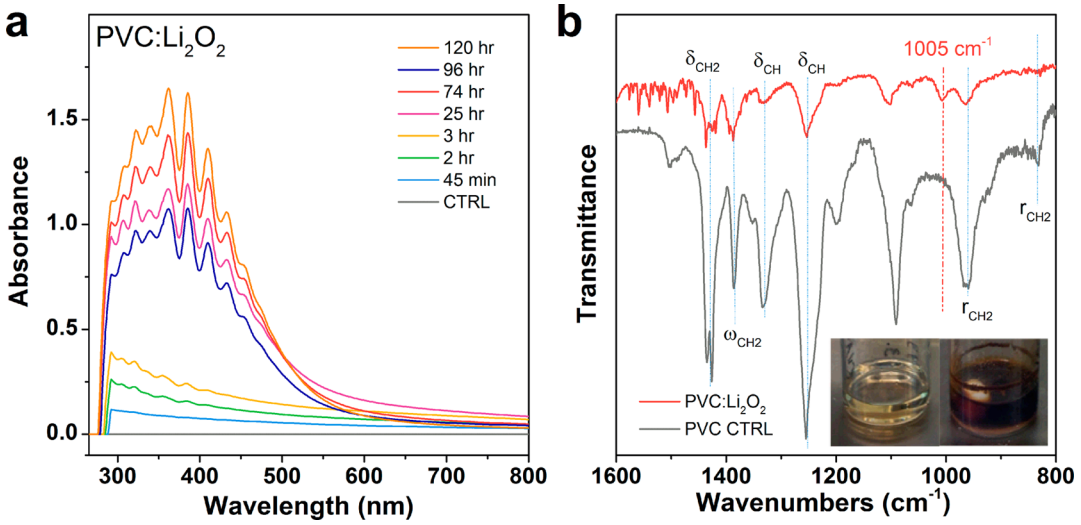


**Figure 5.** (a) UV−vis spectra of the PVC reaction with $Li_2O_2$ as a function of time. The soluble decomposition species that result from PVC degradation increase with time, and absorb over most of the ultraviolet−visible region. (b) FTIR spectra of the PVC:$Li_2O_2$ reaction after 72 h. Inset picture in (b) shows the corresponding color change after reaction. Peak assignments obtained from ref 48, while vibration descriptors are consistent with the notation given in ref 47.

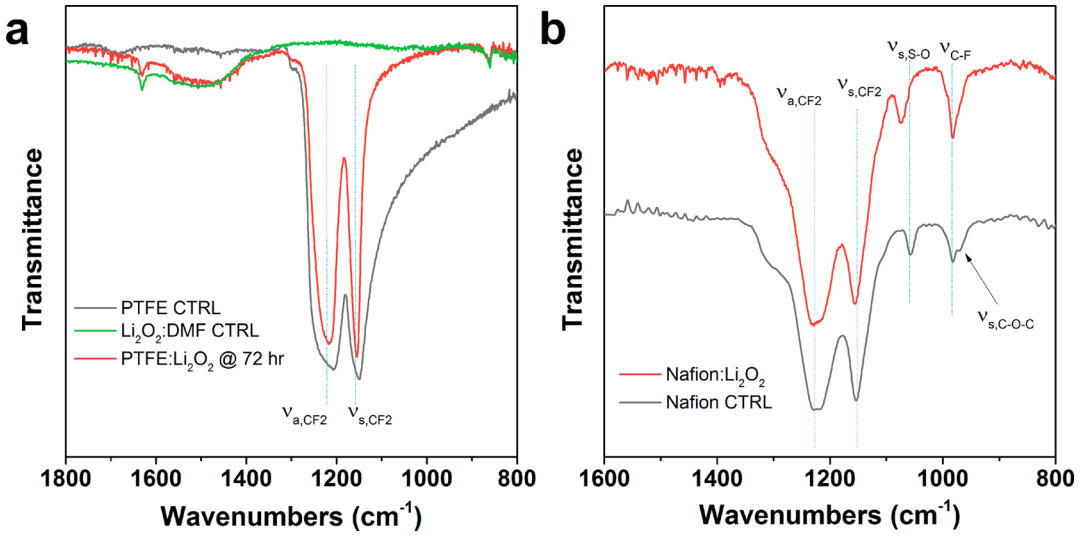


**Figure 6.** FTIR spectra of the mixture of (a) PTFE and (b) Nafion with $Li_2O_2$ after 72 h. Neither PTFE nor Nafion appear reactive with $Li_2O_2$. Peak assignments for (a) and (b) obtained from ref 51, while vibration descriptors are consistent with the notation given in ref 47.

corresponding to an increase in the concentration of soluble conjugated decomposition species resulting from PVC, PVDF, and PVDF-HFP degradation. Possible precipitation of these species led to a decrease in concentration (and absorbance). This is most evident in Figure 5a for the decomposition of PVC as the peak area first increased, and then decreased after longer exposure periods. Interestingly, the UV−vis spectra for the degradation of PVC indicate a range of conjugated species that form, which absorb over most of the UV−vis region.

In the analysis of these halogenated polymers, it is helpful to reference the well-known reactions of alkyl halides. The carbon−halogen (C−Cl, C−F) bond is highly polar due to the significant difference in electronegativity between carbon and the halogens, and this results in an electron-deficient $\alpha$-C atom.[37] Alkyl halides often act as electrophiles and are capable of undergoing two different reactions: (i) nucleophilic substitution at the $\alpha$-C, and (ii) elimination of the $\beta$-H and the halogen to yield an alkene.[37] For PVDF and PVDF-HFP, where fluorine is the halogen, a bimolecular ($S_N2$) substitution of peroxide or any nucleophile at the $\alpha$-C is unfavorable because F is a very poor leaving group. Alkyl fluorides typically do not undergo these $S_N2$-type reactions.[37] In addition, a unimolecular ($S_N1$) substitution is also unlikely because of the poor leaving nature of F, the secondary nature (2°) of the $\alpha$-C, and because the nucleophile $Li_2O_2$ is a strong base.[37] Therefore, an elimination mechanism would be preferred for the reaction of PVDF with $Li_2O_2$, and the PVDF component of PVDF-HFP. A unimolecular (E1) elimination mechanism would be uncompetitive because the first step, which involves F leaving the chain, would be too slow. Therefore, a bimolecular elimination (E2) reaction is favored because of the presence of a strong nucleophile and the highly electron deficient protons, and as shown in Supporting Information Figure S2 begins with the abstraction of a $\beta$-$CH_2$ proton, followed by the formation of an alkene, and then expulsion of the fluorine.[31,37] FTIR spectra[47] of the decomposition products of PVDF and



DOI: 10.1021/cm5040003
Chem. Mater. 2015, 27, 550−561

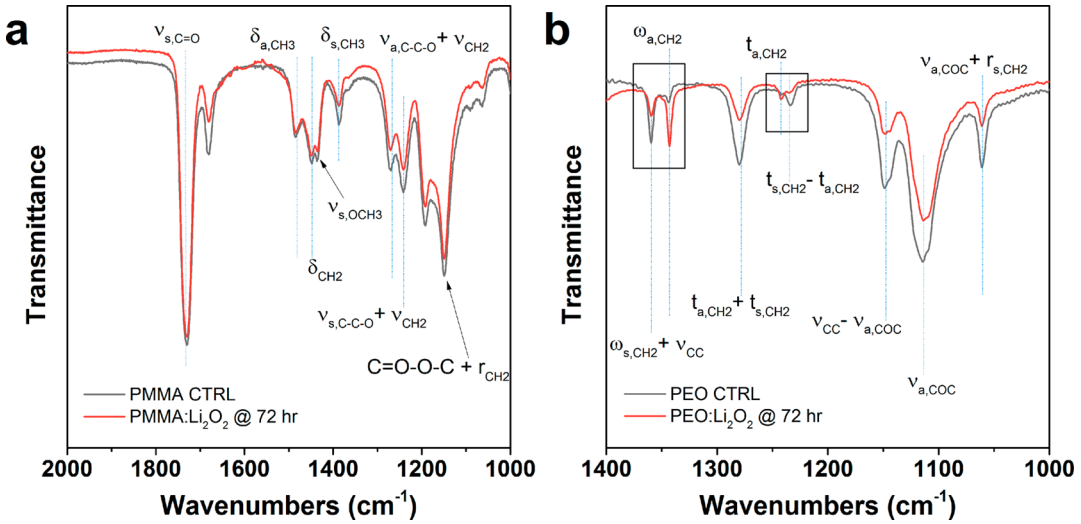


**Figure 7.** FTIR spectra of the mixture of (a) PMMA and (b) PEO with $Li_2O_2$. PMMA appears stable while the intensity of the $CH_2$ vibrations of PEO changes, hinting at a degree of cross-linking within the PEO chains induced by $Li_2O_2$ (boxed section in (b)). Peak assignments for (a) and (b) obtained from refs 57 and 59, respectively, while vibration descriptors are consistent with the notation given in ref 47.

PVDF-HFP in Figure 4c,d support this elimination mechanism and show the rise of the aforementioned alkene C═C stretching vibrations at 1650 $cm^{-1}$ that result from the dehydrofluorination of the PVDF backbone.[31] These C═C vibrations and the formation of the resultant LiF have also been reported by several authors.[29,31,49] The resultant conjugated alkene species is responsible for the observed blackening of the solution, and for the discoloration some have observed when PVDF and PVDF-HFP are used in lithium−air cells.[29,31] It must be mentioned that the presence of two fluorine groups on the polymer's $\alpha$-carbon will make the $\beta$-H protons more electron deficient as compared to, for example, poly(vinyl fluoride) with just one fluorine in its repeat unit.

For PVC, the decomposition mechanism is slightly different. Although the $\alpha$-C of PVC is secondary and also contains a halogen functionality, an $S_N2$-type substitution is possible because Cl is a good leaving group.[37] However, for secondary alkyl halides where a strong base is used, an E2 mechanism dominates like in the fluorinated PVDF and PVDF-HFP, and leads to the elimination of H−Cl (Supporting Information Figures S2, S8) and the formation of alkene species along the polymer backbone.[37,45] Again, these alkene conjugated species are responsible for the color changes, and the FTIR spectra[48] in Figure 5 show the stretch at 1005 $cm^{-1}$ that is specific for long all-trans polyene conjugate species, also observed during the dehydrochlorination of PVC by KOH.[45,50] The UV−vis spectra in Figure 5a are similar to those obtained for PVC that has been degraded thermally and degraded by exposure to potassium *tert*-butoxide, and the general absorption over the UV−vis region is attributed to these long polyene-like moieties.[46] Therefore, it is proposed that PVC, PVDF, and PVDF-HFP undergo dehydrohalogenation processes upon exposure to $Li_2O_2$.

When polymers devoid of hydrogen atoms in their backbone such as fully fluorinated PTFE and Nafion were examined, no reaction with $Li_2O_2$ was observed (Figure 6). The elimination reactions responsible for the degradation of PVC, PVDF, and PVDF-HFP are no longer possible due to the absence of hydrogen atoms that can be abstracted on the polymer chain, and any bimolecular or unimolecular substitutions of peroxide are unfavorable.[37] The FTIR spectra[51] in Figure 6a,b did not show any decomposition products (either alkene or other) for Nafion and PTFE, and no color changes were observed. The new broad peak that did appear in Figure 6a for the PTFE mixture with $Li_2O_2$ was also present in the $Li_2O_2$/DMF control. Nafion was also examined using UV−vis (Supporting Information Figure S3), which revealed no soluble decomposition species. It is important to mention that, although the backbone of commercially sold Nafion often remains the same, the end group varies because of different functional groups introduced to impart solubility properties. If the end-group is reactive with $Li_2O_2$, it is possible for the stability of Nafion to be adversely affected.

Because the fully fluorinated polymers do not appear to react with $Li_2O_2$, the reactive component of the PVDF-HFP copolymer is presumed to be PVDF and not HFP, as HFP is fully fluorinated with no protons on the polymer backbone. As Figure 4a,b shows, the concentration of soluble decomposition species was higher for PVDF than for PVDF-HFP, suggesting PVDF can be more reactive than PVDF-HFP due to the higher fraction or relative concentration of PVDF units in the homopolymer.

**Poly(vinylpyrrolidone).** Poly(vinylpyrrolidone) is another polymer that has been explored for electrolyte systems.[52,53] It has a pyrrolidone side chain on the aliphatic backbone of the polymer. When this polymer was exposed to $Li_2O_2$, a light yellow solution resulted (Supporting Information Figure S4). UV−vis data showed an increase in soluble decomposition species as a function of time, but as compared to the reactive polymers discussed previously, the concentration of soluble decomposition species was much lower (Supporting Information Figure S4c). Therefore, although PVP reacts with $Li_2O_2$, it is a slow reaction, and when the decomposition species were analyzed, no significant changes appeared in the NMR and FTIR spectra (Supporting Information Figures S4a,b).[54] Although the carbonyl group is highly polar, the presence of the nitrogen atom in the ring with its lone pair electrons donates electron density to the carbonyl and reduces the electron deficiency of the $\alpha$-$CH_2$ protons adjacent to the carbonyl.[37] Nucleophilic attack is still possible at the $\alpha$-$CH_2$ position and the carbonyl carbon, and the slight reaction with


DOI: 10.1021/cm5040003
Chem. Mater. 2015, 27, 550−561

$Li_2O_2$ may be due to this attack, but the reaction rate is significantly lower than those discussed above.

**Poly(methyl methacrylate).** Another polymer that has found common utility in gel polymer electrolyte systems for lithium-based batteries is poly(methyl methacrylate) or PMMA.[30,55] A gel can be formed by mixing PMMA powder with organic liquids (or ionic liquid) or polymerizing the monomer MMA in the presence of the ionically conducting organic liquid/ionic liquid.[56] Remarkably, when PMMA was exposed to $Li_2O_2$, it appeared stable, and no discoloration was observed. FTIR (Figure 7a)[57] and NMR (Supporting Information Figure S5)[58] data showed no appearance or disappearance of peaks, and the molecular structure of the polymer before and after $Li_2O_2$ exposure remained intact. However, in the NMR data in Supporting Information Figure S5, an unassigned proton peak at $\delta$ = 3.16 ppm appeared, which may be due to a reactive impurity in PMMA because the polymer backbone and side-chain functionality appear stable.

We can consider the stability of PMMA by simplifying the polymer into an ester-like small molecule that affords us different reaction mechanisms for possible nucleophilic attack by $Li_2O_2$. First, the carbonyl functional group (C═O) is highly polar due to the difference in electronegativity between oxygen and carbon, and like the nitrile carbon and the $\alpha$-C in an alkyl halide, the carbonyl carbon has a partial positive character ($\delta^+$), is acidic, and capable of reacting with nucleophiles.[37] For carbonyl-containing compounds, there are four general reactions that can be anticipated for these systems: (i) $\alpha$ substitution at the carbon $\alpha$ to the carbonyl, (ii) carbonyl condensation between two carbonyls, (iii) nucleophilic addition at the carbonyl carbon, and (iv) nucleophilic acyl substitution at the carbonyl carbon.[37]

At the $\alpha$-C position of PMMA that is attached to the polymer backbone, no hydrogen atom is present. Instead, the $\alpha$-C is substituted with a methyl group that donates electron density to the $\alpha$-C, essentially shutting off any potential reaction mechanism that can occur at that quaternary carbon. Because no $\alpha$-CH is present, the first two reactions listed above are unlikely in PMMA.

Theoretically, the last two reactions listed are possible. Despite the fact that our data show that PMMA is stable, we cannot rule out possible nucleophilic addition (iii) or substitution (iv) at the carbonyl carbon. If PMMA is used in a Li−air cell, strong bases like the superoxide radical anion can possibly add to the carbonyl center, and although this addition is reversible, any impurity such as water present in the cell could lead to further decomposition.[37] This might explain why Nasybulin et al. reported the formation of $Li_2CO_3$ in the mixture of PMMA/$Li_2O_2$/$KO_2$.[32] Also, nucleophilic substitution by a strong base at the carbonyl carbon that leads to elimination of a methoxy anion is possible, but the methoxy anion is a poor leaving group, much worse than fluorine, making this reaction route unfavorable.[37] It is for these reasons we consider PMMA to be stable in the presence of $Li_2O_2$ alone.

**Poly(ethylene oxide).** Unlike the aliphatic (C−C, C−H) backbone polymers such as PAN and PMMA discussed above, whose stability is heavily influenced by the presence and type of functional group, poly(ethylene oxide) (PEO) has an ether backbone with no side-chain functionalities. It is the only polymer studied in this work that, when complexed with a lithium salt, is capable of acting as a good solid-state electrolyte in the absence of liquids. For current lithium−air cells, ether solvents such as dimethoxyethane (DME) and tetraethylene glycol dimethyl ether (TEGDME) have become the solvent of choice,[6,14,60] despite widely varying conclusions regarding their stability.[9,11,61] PEO is essentially a macromolecule of DME, and when exposed to $Li_2O_2$ appears relatively stable (Figure 7b).

Ethers are often highly stable compounds, and, except for possible C−O bond cleavage by strong acids or highly oxidative conditions, are unreactive in the presence of bases, nucleophiles, and many other reagents.[37] This is consistent with our observation that PEO is relatively stable in the presence of $Li_2O_2$. As the FTIR spectrum[59] in Figure 7b shows, no new functional groups are observed after addition of $Li_2O_2$ to the PEO/DMF mixture. However, the change in the ratio of the peaks at 1242 $cm^{-1}$/1234 $cm^{-1}$ and 1360 $cm^{-1}$/1343 $cm^{-1}$ (highlighted in Figure 7b) that correspond to the $CH_2$ stretches indicates that some cross-linking of PEO may have occurred in the presence of $Li_2O_2$. In addition, GPC data showed a 15% increase in the weight-average molecular weight, an increase in the number-average molecular weight by a factor of 3, and a reduction in the polydispersity index by a factor of 2.5, confirming cross-linking of the PEO chains. The NMR spectra show very minor signs of degradation (Supporting Information Figure S6) where a peak associated with lithium formate is observed, an occurrence previously noted in small molecule ethers.[9,60] Furthermore, we must note that ethers can also react with oxygen to form peroxide species.[37] Therefore, future studies would be needed to examine the effect of possible PEO cross-linking on the performance of a lithium−air cell.

**Establishing Reactivity Trends.** The polymers discussed in this work were examined to determine their stability and possible reactivity in the presence of the desired discharge product in a lithium−air cell. However, the goal of this work encompasses more than the study of a small number of polymers; rather, it would be helpful to use the knowledge gained from this subset of polymers to predict the stability of other polymers. This subset of polymers listed in Figure 1 allows us to develop reactivity trends that can prove useful in the selection and utilization of new polymers for lithium−air applications.

UV−vis spectroscopy makes it possible to understand the relative rates of reactivity for the unstable polymers studied. To compare the reactivities of PAN, PVC, PVDF, PVDF-HFP, and PVP, equivalent polymer and $Li_2O_2$ mass concentrations were used (see Experimental Section for more details). Using the absorbance value at $\lambda_{max}$, which corresponds to the concentration of soluble species from polymer degradation, a plot of absorbance versus reaction time (Figure 8) yields a form of kinetic degradation rate curve for each of the polymers. PAN appears to be the most reactive of the polymers studied, and PVP the least. Despite the fact that the aliquot used for the other polymers (PVC, PVDF, PVDF-HFP, and PVP) was 5 times more concentrated than PAN (see Experimental Section), the concentration of PAN decomposition species is still much higher. The order of polymer reactivity with $Li_2O_2$ appears to be as follows: PAN ≫ PVC ≈ PVDF > PVDF-HFP ≫ PVP. At initial reaction times, PVC reacts similarly to PVDF, but, at longer reaction times, PVDF appears more reactive than PVC because the protons in PVDF are more electron-deficient (due to the two fluorine functionalities in each repeat unit) as compared to the protons in PVC. In addition, as mentioned previously, PVDF is more reactive than PVDF-HFP because of the higher PVDF fraction in the homopolymer.

Not surprisingly, at short reaction times, this order of reactivity closely corresponds to the Hammett constants for the


DOI: 10.1021/cm5040003
Chem. Mater. 2015, 27, 550−561

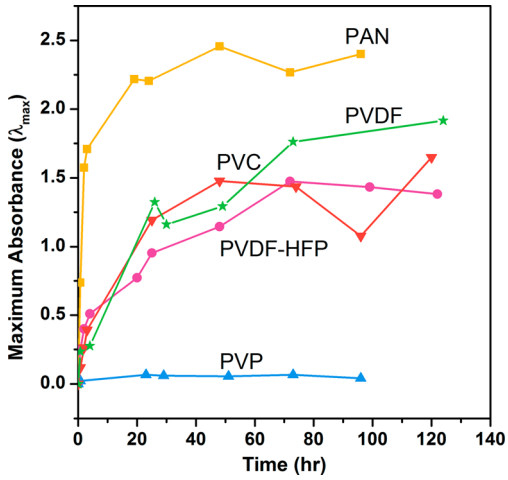


**Figure 8.** Plot of the maximum absorbance ($\lambda_{max}$) at each time point for the different unstable polymer/$Li_2O_2$ mixtures studied. The maximum absorbance corresponds to the soluble decomposition species resulting from polymer degradation. Of the polymers studied, PAN appears to be the most reactive with $Li_2O_2$, while PVP the least. The halogenated polymers have similar reactivities, although at longer times, PVDF appears more reactive than PVC and PVDF-HFP.

different functional groups: PAN (0.56) > PVC (0.37) ≈ PVDF (0.34) > PVP (0.05).[62] This trend is reasonable because it correlates with the electrophilic nature of the functional groups. The higher is the Hammett constant, the more electrophilic and electron withdrawing is the functional group, the more electron-deficient is the polymer chain, and the more reactive the polymer will be with the nucleophilic and electron-rich $Li_2O_2$.[37] However, the electrophilic nature of the functional group on the polymer is not the only parameter that governs reactivity with $Li_2O_2$, especially because PTFE and Nafion share the same functional group as PVDF and PVDF-HFP, but still appear stable. A second parameter, the presence of an $\alpha$- or $\beta$-hydrogen atom adjacent to the electron-withdrawing/electrophilic functional group, also contributes to the polymer's instability.[31] The two parameters that appear to govern reactivity with $Li_2O_2$, and in turn polymer stability in the nucleophilic lithium−air cell environment, are summarized as follows:

(I) The presence of highly electron-withdrawing functional groups on the polymer side chain [−C≡N, −X (F, Cl), $-NO_2$, $-CF_3$] and
(II) If the polymer backbone is aliphatic, the presence of a hydrogen atom that is $\alpha$ or $\beta$ to the electron-withdrawing group.

We propose that these two parameters are important for the stability of the fluorinated polymers (PTFE and Nafion vs PVDF and PVDF-HFP), where the only difference between the two classes is parameter II. For PAN, the presence of the electrophilic nitrile group (parameter I) seems sufficient enough for PAN to react with $Li_2O_2$, especially because nucleophilic attack begins at the nitrile carbon. Replacing the $\alpha$-CH, which is cleaved during PAN reaction with $Li_2O_2$ (Figure 3), with a methyl group might reduce the reactivity of PAN, but will be insufficient to entirely thwart the reaction of PAN. For PVC, the presence of the halide functionality (parameter I) and the adjacent $\alpha$ and $\beta$ hydrogens (parameter II) makes the dehydrochlorination of PVC in the presence of $Li_2O_2$ possible. PVP is much less reactive because the nitrogen donates electron density to the carbonyl side group, while PEO is relatively stable despite possible cross-linking in the presence of $Li_2O_2$ because of the electron-donating nature of the ether functional group.[37]

These guidelines can be used to examine numerous other polymers. For example, a polymer with a nitro functional group ($-NO_2$) or a trifluoromethyl functional group ($-CF_3$) adjacent to an $\alpha$-CH proton will lead to an electron-deficient proton and almost-certain reactivity with $Li_2O_2$. Knowledge of the reactions of small molecules in the presence of bases and nucleophiles should provide additional insight with regards to the chemical stability of polymers for lithium−air.

It is important to note that, although $Li_2O_2$ is used for these polymer screening tests, it may not be the only source of nucleophilic species in a lithium−air cell. It is believed that during cell discharge, superoxide radical anions are formed,[4,17] and they could serve as either a nucleophile or a source of radical species that can propagate polymer decomposition. Therefore, the polymer reactions that occurred in the presence of $Li_2O_2$ may be accelerated in the presence of $O_2^{\bullet-}$ in an actual lithium−air cell. In addition, it will be important to examine the polymers that do appear chemically stable (PTFE, Nafion, PMMA, and PEO) in a lithium−air cell to determine their electrochemical stability in a reduced oxygen environment.

Finally, lithium peroxide size variations[27] and different surface chemistry[63] can also lead to differences between the chemical stability that this work has examined, and what occurs in a fully operating lithium−air cell. Although commercial lithium peroxide is used for this screening study, electrochemically generated lithium peroxide species may be in the form of particles with much smaller dimensions (dependent on discharge capacity)[64] that may increase their surface area and thus reactivity with the polymers studied, and accelerate polymer degradation. In addition, the stability of these polymers upon charging in lithium−air is also of importance, and further studies will be needed to elucidate potential degradation pathways. Continued degradation of the polymer that serves as an electrolyte or as a binder will contribute to poor rate capabilities of lithium−air cells, poor round-trip efficiencies, and a much shorter cell lifetime.[29]

## CONCLUSIONS

Using commercial lithium peroxide as a screening tool, we have examined the stability of polymers that have been commonly used for lithium-based battery applications. The polymers PAN, PVC, PVDF, PVDF-HFP, and PVP react with $Li_2O_2$ and are unstable. The polymers PMMA, PTFE, and Nafion appear chemically stable in the presence of $Li_2O_2$. PEO appears relatively stable, but may undergo some chemical cross-linking. Using tools such as UV−vis, NMR, FTIR, and GPC, the decomposition species were characterized to determine the modes of degradation. Two parameters seem to govern the stability of the polymers studied: (i) the presence of highly electron-withdrawing/electrophilic functional groups on the polymer side chain, and (ii) the presence of hydrogen atoms that are adjacent to the aforementioned electron-withdrawing groups. Lithium peroxide or any oxygen free-radical species or nucleophile in a lithium−air cell can attack these unstable polymers, leading to polymer decomposition that will negatively affect the chemistry and long-term performance of a lithium−air cell. Finally, these studied polymers provide invaluable insight into the general stability of polymers and the correlation between polymers and their small organic molecule


DOI: 10.1021/cm5040003
Chem. Mater. 2015, 27, 550−561

counterparts. Understanding the general reactivity of functional groups with bases and nucleophiles will be important in the selection and development of new polymers for lithium−air applications.

## ■ ASSOCIATED CONTENT

### Supporting Information

Properties of the polymers studied, and the FTIR, NMR, and UV−vis spectra of the polymer reactivity studies with $Li_2O_2$. This material is available free of charge via the Internet at http://pubs.acs.org.

## ■ AUTHOR INFORMATION


### Corresponding Authors

*E-mail: shaohorn@mit.edu.

*E-mail: hammond@mit.edu.


### Notes

The authors declare no competing financial interest.

## ■ ACKNOWLEDGMENTS

This work was supported by the Samsung Advanced Institute of Technology (SAIT), and the facilities at the Koch Institute for Integrative Cancer Research at MIT. We also thank the Institute for Soldier Nanotechnologies (ISN) at MIT for use of their GPC. C.V.A. would like to acknowledge the GEM Fellowship, and support by the Department of Defense (DoD) through the National Defense Science & Engineering Graduate (NDSEG) Fellowship Program.

## ■ ABBREVIATIONS

PAN, poly(acrylonitrile); PEO, poly(ethylene oxide); PMMA, poly(methyl methacrylate); PTFE, poly(tetrafluoroethylene); PVC, poly(vinyl chloride); PVDF, poly(vinylidene fluoride); PVDF-HFP, poly(vinylidene fluoride-*co*-hexafluoropropylene); PVP, poly(vinylpyrrolidone); DMF, *N*,*N*-dimethylformamide; DMAc, *N*,*N*-dimethylacetamide; DMSO, dimethyl sulfoxide; TMS, tetramethylsilane

## ■ REFERENCES


(1) Bruce, P. G.; Freunberger, S. A.; Hardwick, L. J.; Tarascon, J.-M. *Nat. Mater.* **2011**, *11*, 19−29.

(2) Scrosati, B.; Hassoun, J.; Sun, Y.-K. *Energy Environ. Sci.* **2011**, *4*, 3287−3295.

(3) Girishkumar, G.; McCloskey, B.; Luntz, A.; Swanson, S.; Wilcke, W. *J. Phys. Chem. Lett.* **2010**, *1*, 2193−2203.

(4) Lu, Y.-C.; Gallant, B. M.; Kwabi, D. G.; Harding, J. R.; Mitchell, R. R.; Whittingham, M. S.; Shao-Horn, Y. *Energy Environ. Sci.* **2013**, *6*, 750−768.

(5) Lu, Y.-C.; Gasteiger, H. A.; Parent, M. C.; Chiloyan, V.; Shao-Horn, Y. *Electrochem. Solid-State Lett.* **2010**, *13*, A69−A72.

(6) Mitchell, R. R.; Gallant, B. M.; Thompson, C. V.; Shao-Horn, Y. *Energy Environ. Sci.* **2011**, *4*, 2952−2958.

(7) Kwabi, D.; Ortiz-Vitoriano, N.; Freunberger, S.; Chen, Y.; Imanishi, N.; Bruce, P.; Shao-Horn, Y. *MRS Bull.* **2014**, *39*, 443−452.

(8) Gallagher, K. G.; Goebel, S.; Greszler, T.; Mathias, M.; Oelerich, W.; Eroglu, D.; Srinivasan, V. *Energy Environ. Sci.* **2014**, *7*, 1555−1563.

(9) Freunberger, S. A.; Chen, Y.; Drewett, N. E.; Hardwick, L. J.; Bardé, F.; Bruce, P. G. *Angew. Chem., Int. Ed.* **2011**, *50*, 8609−8613.

(10) Freunberger, S. A.; Chen, Y.; Peng, Z.; Griffin, J. M.; Hardwick, L. J.; Bardé, F.; Novák, P.; Bruce, P. G. *J. Am. Chem. Soc.* **2011**, *133*, 8040−8047.

(11) McCloskey, B.; Speidel, A.; Scheffler, R.; Miller, D.; Viswanathan, V.; Hummelshøj, J.; Nørskov, J.; Luntz, A. *J. Phys. Chem. Lett.* **2012**, *3*, 997−1001.

(12) Lu, Y.-C.; Kwabi, D. G.; Yao, K. P.; Harding, J. R.; Zhou, J.; Zuin, L.; Shao-Horn, Y. *Energy Environ. Sci.* **2011**, *4*, 2999−3007.

(13) Gallant, B. M.; Mitchell, R. R.; Kwabi, D. G.; Zhou, J.; Zuin, L.; Thompson, C. V.; Shao-Horn, Y. *J. Phys. Chem. C* **2012**, *116*, 20800−20805.

(14) Jung, H.-G.; Hassoun, J.; Park, J.-B.; Sun, Y.-K.; Scrosati, B. *Nat. Chem.* **2012**, *4*, 579−585.

(15) Lu, Y.-C.; Gasteiger, H. A.; Crumlin, E.; McGuire, R.; Shao-Horn, Y. *J. Electrochem. Soc.* **2010**, *157*, A1016−A1025.

(16) Laoire, C. O.; Mukerjee, S.; Abraham, K.; Plichta, E. J.; Hendrickson, M. A. *J. Phys. Chem. C* **2010**, *114*, 9178−9186.

(17) Sharon, D.; Etacheri, V.; Garsuch, A.; Afri, M.; Frimer, A. A.; Aurbach, D. *J. Phys. Chem. Lett.* **2012**, *4*, 127−131.

(18) Peng, Z.; Freunberger, S. A.; Chen, Y.; Bruce, P. G. *Science* **2012**, *337*, 563−566.

(19) Chen, Y.; Freunberger, S. A.; Peng, Z.; Fontaine, O.; Bruce, P. G. *Nat. Chem.* **2013**, *5*, 489−494.

(20) Ottakam Thotiyl, M. M.; Freunberger, S.; Peng, Z.; Chen, Y.; Liu, Z.; Bruce, P. *Nat. Mater.* **2013**, *12*, 1050.

(21) Bryantsev, V. S.; Giordani, V.; Walker, W.; Blanco, M.; Zecevic, S.; Sasaki, K.; Uddin, J.; Addison, D.; Chase, G. V. *J. Phys. Chem. A* **2011**, *115*, 12399−12409.

(22) Hassoun, J.; Croce, F.; Armand, M.; Scrosati, B. *Angew. Chem., Int. Ed.* **2011**, *50*, 2999−3002.

(23) Aurbach, D.; Daroux, M.; Faguy, P.; Yeager, E. *J. Electroanal. Chem. Interfacial Electrochem.* **1991**, *297*, 225−244.

(24) McCloskey, B.; Bethune, D.; Shelby, R.; Girishkumar, G.; Luntz, A. *J. Phys. Chem. Lett.* **2011**, *2*, 1161−1166.

(25) Chen, Y.; Freunberger, S. A.; Peng, Z.; Bardé, F.; Bruce, P. G. *J. Am. Chem. Soc.* **2012**, *134*, 7952−7957.

(26) Sharon, D.; Afri, M.; Noked, M.; Garsuch, A.; Frimer, A. A.; Aurbach, D. *J. Phys. Chem. Lett.* **2013**, *4*, 3115−3119.

(27) Kwabi, D. G.; Batcho, T. P.; Amanchukwu, C. V.; Ortiz-Vitoriano, N. P.; Hammond, P. T.; Thompson, C. V.; Shao-Horn, Y. *J. Phys. Chem. Lett.* **2014**.

(28) Li, F.; Kitaura, H.; Zhou, H. *Energy Environ. Sci.* **2013**, *6*, 2302−2311.

(29) Jung, K.-N.; Lee, J.-I.; Jung, J.-H.; Shin, K.-H.; Lee, J.-W. *Chem. Commun.* **2014**, *50*, 5458−5461.

(30) Manuel Stephan, A. *Eur. Polym. J.* **2006**, *42*, 21−42.

(31) Black, R.; Oh, S. H.; Lee, J.-H.; Yim, T.; Adams, B.; Nazar, L. F. *J. Am. Chem. Soc.* **2012**, *134*, 2902−2905.

(32) Nasybulin, E.; Xu, W.; Engelhard, M. H.; Nie, Z.; Li, X. S.; Zhang, J.-G. *J. Power Sources* **2013**, *243*, 899−907.

(33) Itkis, D. M.; Semenenko, D. A.; Kataev, E. Y.; Belova, A. I.; Neudachina, V. S.; Sirotina, A. P.; Hävecker, M.; Teschner, D.; Knop-Gericke, A.; Dudin, P. *Nano Lett.* **2013**, *13*, 4697−4701.

(34) Manuel Stephan, A.; Nahm, K. *Polymer* **2006**, *47*, 5952−5964.

(35) Abraham, K.; Jiang, Z. *J. Electrochem. Soc.* **1996**, *143*, 1−5.

(36) Choe, H.; Carroll, B.; Pasquariello, D.; Abraham, K. *Chem. Mater.* **1997**, *9*, 369−379.

(37) McMurry, J. *Organic Chemistry*; Brooks/Cole Cengage Learning: Boston, MA, 2012.

(38) Coleman, M.; Petcavich, R. *J. Polym. Sci., Polym. Phys. Ed.* **1978**, *16*, 821−832.

(39) Shimada, I.; Takahagi, T.; Fukuhara, M.; Morita, K.; Ishitani, A. *J. Polym. Sci., Part A: Polym. Chem.* **1986**, *24*, 1989−1995.

(40) Varma, D. S.; Needles, H. L.; Cagliostro, D. E. *Ind. Eng. Chem. Prod. Res. Dev.* **1981**, *20*, 520−524.

(41) Verneker, V. P.; Shaha, B. *Macromolecules* **1986**, *19*, 1851−1856.

(42) Mailhot, B.; Gardette, J.-L. *Polym. Degrad. Stab.* **1994**, *44*, 223−235.

(43) Chen, J.; Harrison, I. *Carbon* **2002**, *40*, 25−45.

(44) Xu, W.; Viswanathan, V. V.; Wang, D.; Towne, S. A.; Xiao, J.; Nie, Z.; Hu, D.; Zhang, J.-G. *J. Power Sources* **2011**, *196*, 3894−3899.

(45) Bowley, H. J.; Gerrard, D. L.; Maddams, W. F. *Makromol. Chem.* **1985**, *186*, 707−714.

(46) Bowley, H. J.; Gerrard, D. L.; Maddams, W. F.; Paton, M. R. *Makromol. Chem.* **1985**, *186*, 695−705.




DOI: 10.1021/cm5040003
*Chem. Mater.* 2015, 27, 550−561

(47) Kobayashi, M.; Tashiro, K.; Tadokoro, H. *Macromolecules* **1975**, *8*, 158−171.
(48) Krimm, S.; Folt, V.; Shipman, J.; Berens, A. *J. Polym. Sci., Part A: Gen. Pap.* **1963**, *1*, 2621−2650.
(49) Younesi, R.; Hahlin, M.; Treskow, M.; Scheers, J.; Johansson, P.; Edström, K. *J. Phys. Chem. C* **2012**, *116*, 18597−18604.
(50) Mano, V.; Felisberti, M.; De Paoli, M.-A. *Macromolecules* **1997**, *30*, 3026−3030.
(51) Liang, Z.; Chen, W.; Liu, J.; Wang, S.; Zhou, Z.; Li, W.; Sun, G.; Xin, Q. *J. Membr. Sci.* **2004**, *233*, 39−44.
(52) Abraham, K.; Alamgir, M. *J. Electrochem. Soc.* **1990**, *137*, 1657−1658.
(53) Abraham, K.; Alamgir, M. *Chem. Mater.* **1991**, *3*, 339−348.
(54) Ghosh, G.; Kanti Naskar, M.; Patra, A.; Chatterjee, M. *Opt. Mater.* **2006**, *28*, 1047−1053.
(55) Adebahr, J.; Byrne, N.; Forsyth, M.; MacFarlane, D.; Jacobsson, P. *Electrochim. Acta* **2003**, *48*, 2099−2103.
(56) Susan, M. A. B. H.; Kaneko, T.; Noda, A.; Watanabe, M. *J. Am. Chem. Soc.* **2005**, *127*, 4976−4983.
(57) Brinkhuis, R.; Schouten, A. *Macromolecules* **1991**, *24*, 1496−1504.
(58) Nishioka, A.; Watanabe, H.; Yamaguchi, I.; Shimizu, H. *J. Polym. Sci.* **1960**, *45*, 232−234.
(59) Yoshihara, T.; Tadokoro, H.; Murahashi, S. *J. Chem. Phys.* **1964**, *41*, 2902−2911.
(60) Yao, K. P.; Lu, Y.-C.; Amanchukwu, C. V.; Kwabi, D. G.; Risch, M.; Zhou, J.; Grimaud, A.; Hammond, P. T.; Bardé, F.; Shao-Horn, Y. *Phys. Chem. Chem. Phys.* **2014**, *16*, 2297−2304.
(61) Schwenke, K. U.; Meini, S.; Wu, X.; Gasteiger, H. A.; Piana, M. *Phys. Chem. Chem. Phys.* **2013**, *15*, 11830−11839.
(62) Hansch, C.; Leo, A.; Taft, R. *Chem. Rev.* **1991**, *91*, 165−195.
(63) Gallant, B. M.; Kwabi, D. G.; Mitchell, R. R.; Zhou, J.; Thompson, C. V.; Shao-Horn, Y. *Energy Environ. Sci.* **2013**, *6*, 2518−2528.
(64) Lim, H. D.; Song, H.; Kim, J.; Gwon, H.; Bae, Y.; Park, K. Y.; Hong, J.; Kim, H.; Kim, T.; Kim, Y. H. *Angew. Chem., Int. Ed.* **2014**, *53*, 3926−3931.


DOI: 10.1021/cm5040003
*Chem. Mater.* 2015, 27, 550−561